MULTI-PASSAGE GASDYNAMIC INTERACTIONS IN WAVE ROTOR

Koji OKAMOTO, Toshio NAGASHIMA, and Susumu TERAMOTO
Department of Aeronautics and Astronautics,
School of Engineering, The University of Tokyo
7-3-1, Hongo, Bunkyo-ku, Tokyo, JAPAN

Keywords: *wave rotor, shock waves, unsteady flow*

Abstract

In the wave rotor design, significant importance has to be stressed upon the exact estimation of pressure wave generation and propagation, which is far more difficult than that in ordinary shock tube operation due to complexity of inner flow wave dynamics. In the present paper, some of our detailed investigations following 2D numerical simulation and experimental visualization are introduced to clarify several interesting aspects of the wave rotor inner flow phenomena, including the interaction effect of adjacent passages. The propagating velocity of pressure waves was shown to be also much affected by the gradual passage opening effect, that is, the cells getting gradually opened/closed relative to the ports. Both numerical and experimental results showed good agreement. Another finding was a mechanism of extra pressure wave generation due to the leak flow across adjacent cells through the clearance region, where the rotor cell entrance/exit is sliding in the circumferential direction against the end wall where the intake/exhaust ports are accommodated. The latter extra pressure wave amplitude becomes almost as large as that of the secondary (reflection) shock wave, thus, depending upon the clearance size, yields significant influence to the air compression process.

1 Introduction

Wave Rotor is a device of full potential to improve the gas turbine performance drastically, when synthesized as a topping cycle [1]. The intention of its use for aero-engines is not new, but it has been known as a dynamic pressure wave exchanger with various ways of application like diesel superchargers, wave engines, pressure-gain combustors, air-cycle refrigeration, etc.[2] Although the wave rotor research efforts tend towards machines of larger power size, it should be nowadays noticed that distributed or mobile micro innovative power or energy system is getting popular and of increasing demand, whilst the performance of gas turbines are very much deteriorated if conventional design methodology for large turbo-machines is straightly adopted for miniaturization, so that the mechanical blade work might be efficiently replaced by wave dynamic power conversion devises. The direction of research for Micro Wave Rotors is therefore needed to be further explored [8][9]. As for its structure, Wave Rotor consists of a rotor and ducts (Fig.1), wherein the rotor has many straight passages called “cells”, so that the

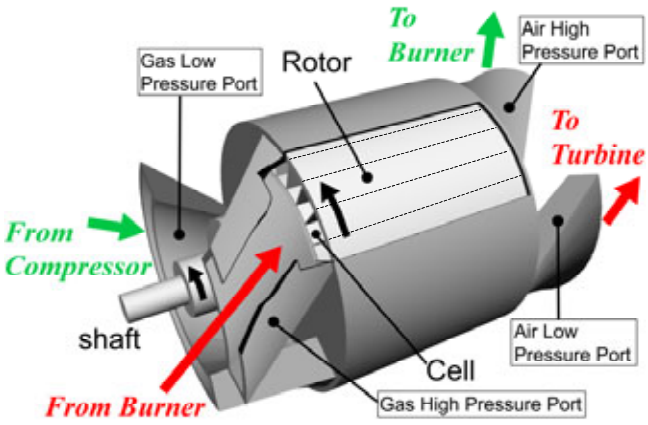

Fig.1 Wave Rotor

ducts called “ports” are connected to the gas turbine components, charging or discharging the combustion gas or fresh air with appropriate schedule.

Fig.2 shows an example of compression process of wave rotor, in which the pressure waves are drawn with characteristic lines (the axes in this figure mean the cell length x and rotational angle θ or time.) At the beginning of the cycle (at the top in the figure), the cell is filled with low pressure air from the compressor. Gas-HP is the port to charge the combustion gas from the burner, and the pressure ratio between gas and air being more than 2. A shock wave (primary shock wave) is therefore generated when the cell is opened to the Gas-HP. The primary shock wave is reflected at the end of the cell, and another shock wave (secondary shock wave) is generated. Air-HP is opened to the cell just after this shock wave reflection, so that high pressure air in the cell, which is compressed by these two shock waves, flows out to the Air-HP. When the secondary shock wave reaches to the end of the cell, Gas-HP is closed and an expansion wave is generated by inertia of the inflow gas. And the Air-HP is closed when this expansion wave reaches to the end of the cell.

As seen in this compression process, the timings of ports’ opening and closing are very important in the wave rotor operation. Therefore, it is indispensable to predict the propagating velocity of these pressure waves in designing a wave rotor. It should be pointed out that exact

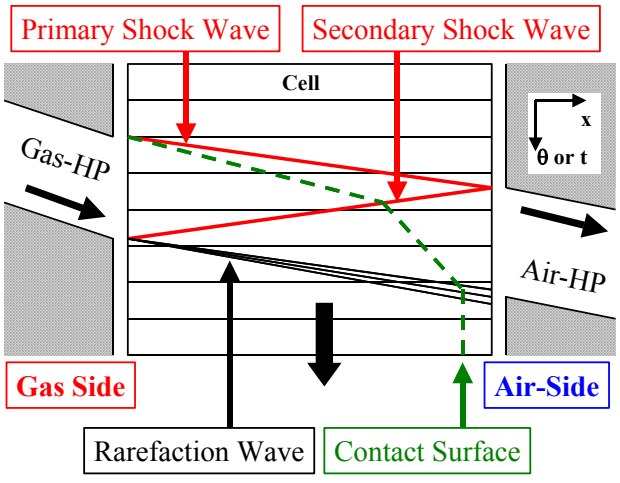

Fig.2 Wave Rotor Compression Process

estimation of the propagating velocity becomes more difficult task than in ordinary shock tube operation, since the inner flow dynamics is far different from the treatment in accordance with the method of characteristics. Many studies have been so far conducted to achieve an appropriate wave rotor designing, which may be roughly classified into

1. Analytical Cycle Calculation [1][3][4][5][6]
2. 1D Over- all Simulation [7][8][9]
3. CFD Analysis (2D or 3D) [10][11][12][13]
4. Experiment [12][13][14]

According to the experimental study in NASA [14], there are three dominant factors in the wave rotor performance estimation, that is,

- Gradual Passage Opening Effect
- Viscosity
- Leakage (Clearance)

“Gradual Passage Opening Effect” means that the cells are gradually opened and closed to the ports, in contrast to instantaneously broken of a diaphragm in shock tube operation, which may lead to a large influence upon the process of wave generation, growth and propagation.

Three factors above are characterized by corresponding non-dimensional parameters below:

- Gradual Passage Opening Effect

$$\tau \equiv \frac{Passage - Opening - Time}{Wave - Travel - Time} = \left(\frac{W_{cell}}{V_{rot}}\right)\cdot\left(\frac{a}{L_{cell}}\right)$$

- Viscosity (Wall Friction)

$$F \equiv \frac{\sqrt{\nu \cdot L_{cell}/a}}{D_h}$$

- Leakage

$$G \equiv \frac{2\cdot\delta_{clr}}{H}$$

Nomenclature

W_{cell}	: Cell Width
V_{rot}	: Peripheral Velocity of rotor
a	: Sound Speed
L_{cell}	: Cell Length
ν	: Kinetic Viscosity
D_h	: Hydraulic Diameter of a cell
δ_{clr}	: clearance
H	: Cell Height

With these parameters, the efficiency of a wave rotor can be estimated roughly as,

$$\eta = b_0 + b_1 \cdot G + b_2 \cdot \tau^2 + b_3 \cdot F^2 + b_4 \cdot \tau \cdot F$$

Here, b_i is a coefficient, which is determined according to the operating condition. The value of each parameter is less than 1.0, therefore the leakage effect has the largest influence on the wave rotor performance among these three factors.

The definitions of parameters above show that the gradual passage opening effect is closely related to the cell width, whilst the leakage effect is closely related to the clearance. In the present study, therefore, the cell width and clearance were chosen to be variable parameters of checking the due influences.

Both 2D numerical simulation and experimental visualization were employed for investigating the pressure wave dynamics in the compression process [12][13]. First, a single cell analysis was tried to cross check the agreement between experimental results and numerical simulation to measure the gradual passage opening effect. After that, detailed observation was attempted to reveal how the inner flow dynamics are affected by the gradual passage opening and leakage effects.

2 Present Study

2.1 Experimental Visualization

To visualize the inner flow of a wave rotor, a test equipment with a new concept was adopted in the experiment (Fig.3). In this design, the cell

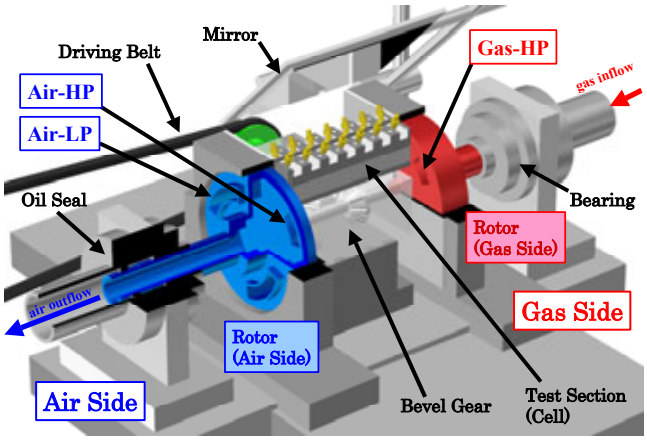

Fig.3 Equipment for Visualization

is fixed stationary, while the ports are rotating, so that the reflecting schlieren method and the direct wall static pressure measurement can be employed. A care is therefore needed that the "rotors" (red and blue parts) in Fig.3 mean the rotating ports to charge / discharge the working gas. These rotors are connected to the bevel gear, and driven by an electric motor.

The design particulars of this equipment are,

Cell Length	: 186mm
Cell Height	: 16mm
Cell Width	: 8mm or 16mm
Rotor Mean Radius	: 60mm
Rotating Speed	:4200rpm
Pressure Ratio of Gas-HP and Air-LP	: 2.6
Clearance	: Variable

Here, compressed air with room temperature was supplied to Gas-HP, though it will be called "gas" for simple description. Also, the test section can be changed according to the objectives.

2.2 Numerical Flow Simulation

2-D numerical analyses at the mean radius plane (i.e. developed in the cell axis and rotating directions) were attempted here. The governing equations are 2D Navier-Stokes equations with laminar viscosity. The solution scheme is based upon Finite Difference Method discretization, incorporating Chakravathy-Osher's 3rd order upwind TVD scheme with the van Leer's differentiable limitter. As for the time integration, the Jameson-Baker's four-stage

Runge-Kutta scheme (fourth-order accuracy) was adopted. Presently, the attention was focused on the dynamics associated with "primary" and "secondary" shock waves during the compression process.

As for the calculation regions, the basic design is the same as the test section in the experiment. Also the inflow and outflow conditions were set to be the same as the experiment applying the characteristic line method with Riemann invariance to treat the pressure wave reflection precisely at the end of the cells.

3 Results

3.1 Wave Visualization

A world-first achieved kind of experimental visualization in Fig.4 was made possible owing to innovative idea of using the inverse rotor/port configuration described in the previous section 2.1. As observed from these Schlieren pictures, the primary shock wave does not appear at DT=100μs, because the density gradient at the shock wave is not strong enough at this moment. "DT" here indicates the time elapsed from the moment when Gas-HP starts opening upwards from the bottom at the cell end. Fig.5 shows computed non-dimensional density contours for the corresponding single passage case of 8mm cell width. In this calculation, the clearance effect was not considered. When Gas-HP started opening, compression wave and contact surface were generated and propagated to the air side, gradually strengthened after all into "Primary shock wave". As for the contact surface, a region called "Captured gas" was formed near the upper corner of the cell entrance (DT=200μs). Upon the primary shock wave reflection at the end of the air side, the secondary shock wave was generated and propagated to the gas side against the incoming flow to interact with the contact surface. When the secondary shock wave reached to the end of the gas side, Gas-HP started closing to result in the appearance of a low pressure area. More detailed descriptions including the comparison

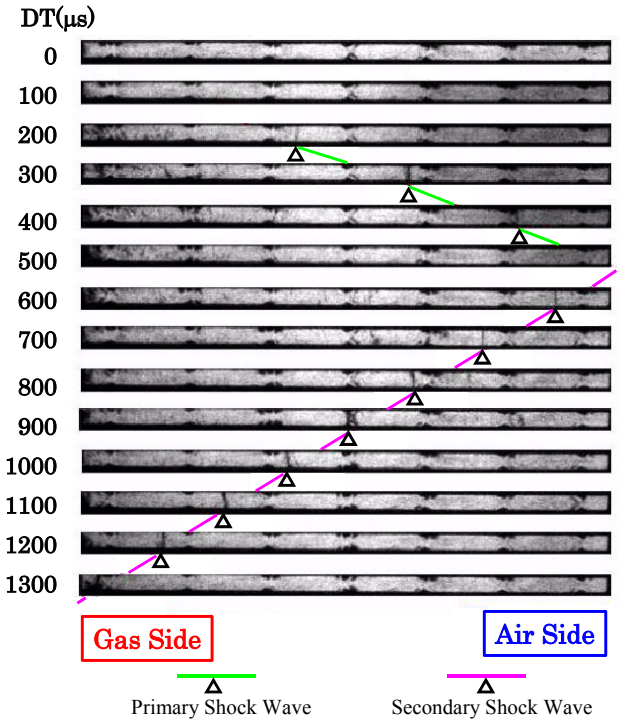

Fig.4 Schlieren Pictures (Single Passage Case)

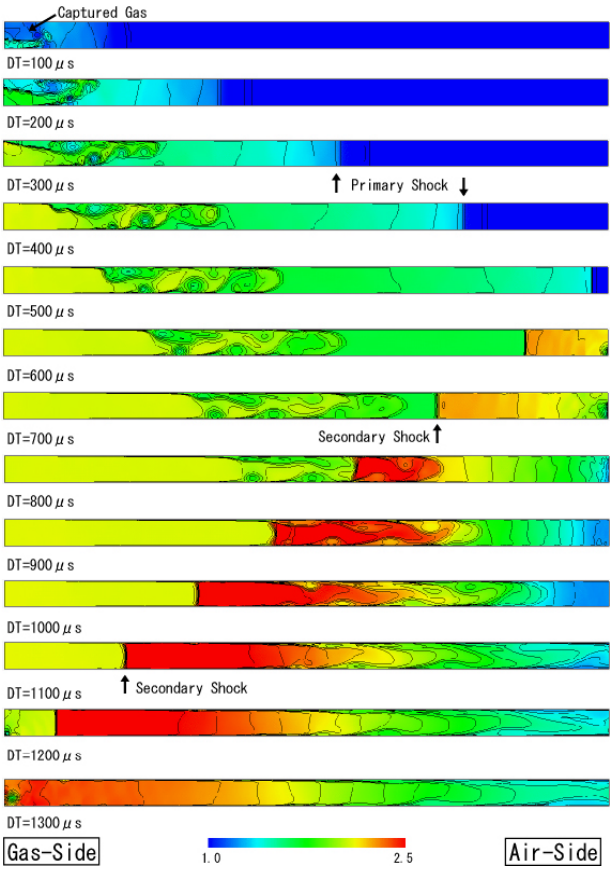

Fig.5 Density Contour of Single Passage Case (without clearance)

between numerical and experimental results are explained in [13]. Table 1 summarizes an example of principal data showing the average propagating velocity of the shock waves, in which the result of analysis for the leak flow effect through a clearance of 0.5mm was also added for examination. Propagation speed of the primary shock wave is apparently not affected, whilst that of the secondary shock wave is affected by the leakage. The above findings were also confirmed by experiments [13].

Table 1 Propagating Velocities of Shock Waves

	Primary Shock Wave	Secondary Shock Wave
Experiment	358 m/s	218 m/s
Without Leakage effect	368 m/s	253 m/s
With Leakage effect	368 m/s	236 m/s

3.2 Gradual Passage Opening Effect

The gradual passage opening effect was investigated by comparing the cases of cell width between 8mm and 16mm. All design and operating conditions except for the cell width were completely fixed to the same (the clearance effect is not considered), therefore, the value of τ becomes doubled, which should yield any difference due to the larger "gradual passage opening effect" [12].

Fig.5 and Fig.6 show the corresponding numerical results, wherein the primary shock wave in 16mm width is seen to be not very distinguishably identified as that in 8mm width. This effect can be also noticed in the wall static pressure traces which were plotted from both numerical and experimental results [12]. It is observed that, in the wider 16mm case, the contact surface shape becomes more complicated, so that the secondary shock wave experiences much interference with the vortices thereupon, as markedly indicated in the shock wave pattern of the experimental schlieren picture of Fig.7.

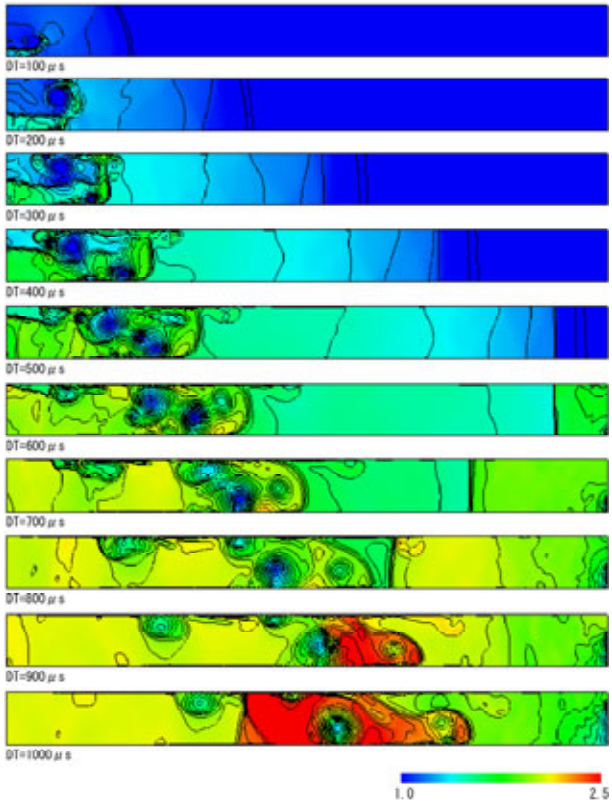

Fig.6 Density Contour (Cell Width 16mm)

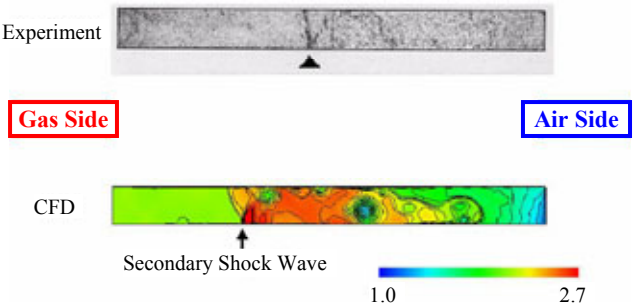

Fig.7 Interference between the secondary shock wave and contact surface

3.3 Multi Passage Interactions

The leakage discussed so far concerns the flow to the outside in general, however, the actual flow in the clearance region has to be differentiated depending upon either radial or circumferential direction. The flow in the radial direction is the leakage to the outside, whilst the flow in the circumferential direction causes the multi passage interaction, that is, across the adjacent cells.

Having established the present numerical as well as experimental methodology, the

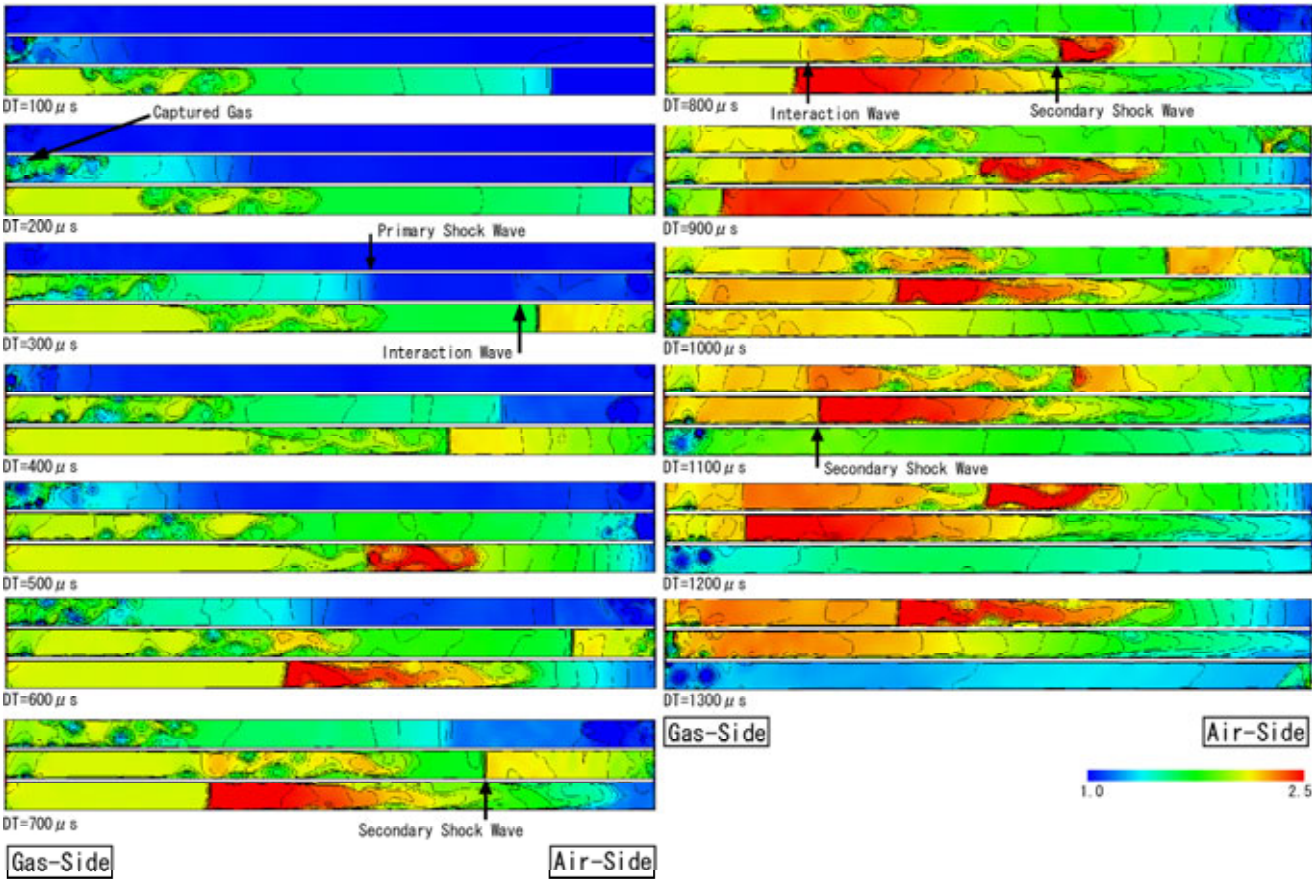

Fig.8 Density Contour (3-Passage)

investigation by employing 3 passages model was conducted to clarify the multi passage interactions as well as the leak flow effect. It should be mentioned that careful comparison of the data from numerical simulations between 3 and 5 passage models has already confirmed the validity of treating the multi passage interaction phenomena based upon the 3 passage model.

Fig.8 shows the result for a case of 0.5mm clearance. In this figure, the datum of DT is notified at the instant when Gas-HP starts opening with respect to the middle cell. By comparing with Fig.5, an extra wave that is herein named “interaction wave” is now observed to be generated in the middle cell, and it propagates to the gas side. The generation process of this interaction wave is detailed in Fig.9, which shows the density contour near the cell end when the primary shock wave is reflected in the bottom cell. At this moment, the pressure in the bottom cell becomes raised, while the pressure in the middle cell is still low,

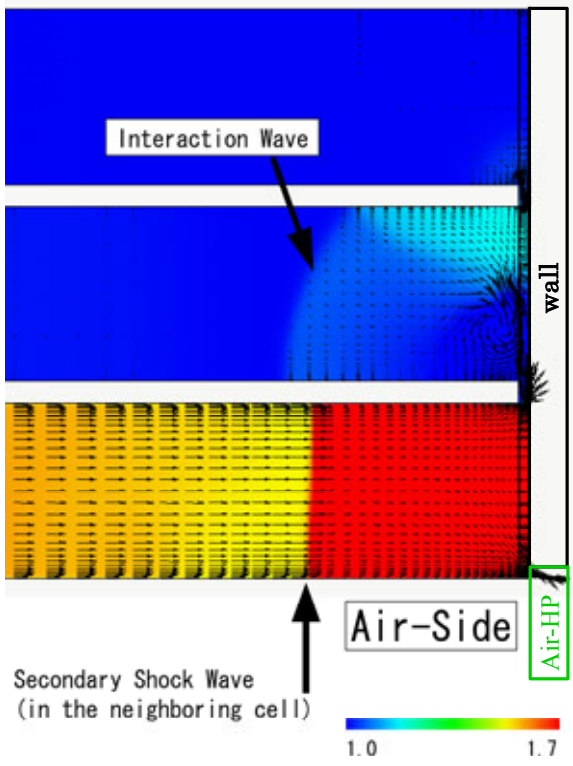

Fig.9 Interaction Wave

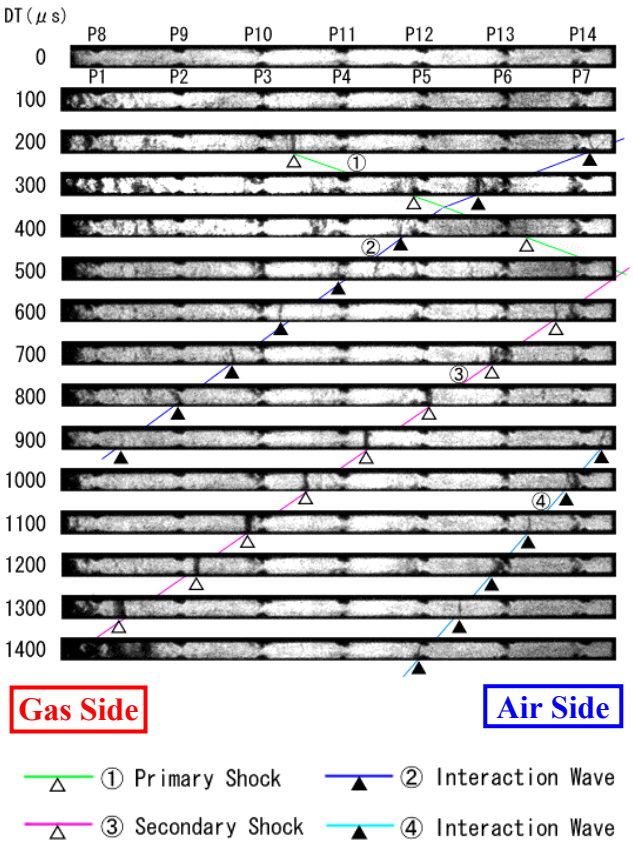

Fig.10 Schlieren Pictures
(Multi Passage, 0.5mm Clearance)

since the ports are moving upward, causing a phase lag in the opening time, so that the bottom cell is opened to each port always earlier than the middle cell. Therefore, the high pressure air rushes into the middle cell from the bottom cell through the clearance region, and a compression wave gets generated. This phenomenon also becomes evident from 3-passage experiment as vividly observed in the schlieren pictures in Fig.10.

To discuss the leakage effect, 1.0mm clearance was also tried and compared with the 0.5mm clearance. Fig.11 shows an example of experimentally obtained time traces of the wall static pressure. With increasing the clearance, the strength of secondary shock wave is weakened, so that, in the case of 1.0mm clearance, for instance, the strength of secondary shock wave becomes almost the same as that of the interaction wave. This phenomenon was again shown in both numerical and experimental results. It can be

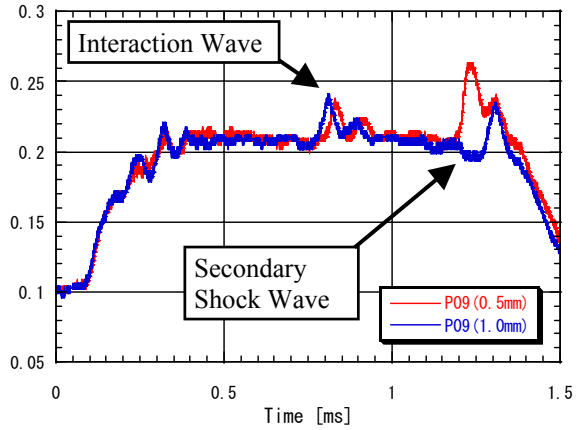

Fig.11 Time Trace of Wall Static Pressure (Experiment)

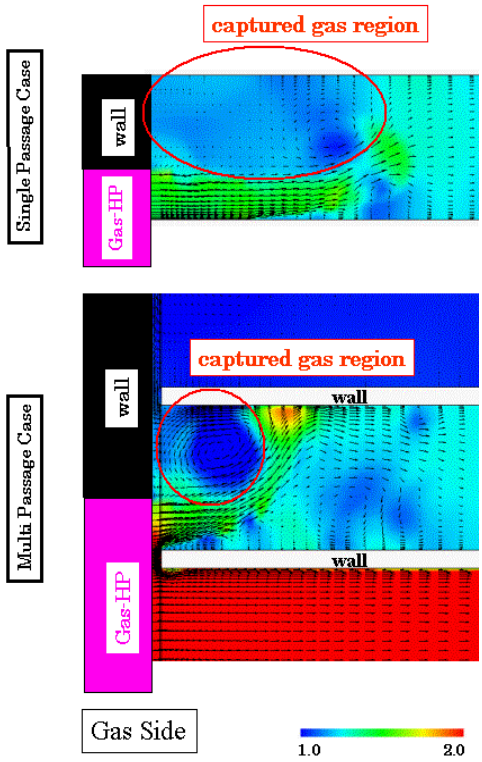

Fig.12 Inflow Difference

concluded that the interaction effect is not negligible when the clearance gets large [13].

It is also noticeable that the state of contact surface is very different from that in the single passage, owing to the difference in the inflow angle or incidence at the beginning of Gas-HP opening (Fig.12). In the single passage case, the inflow direction was almost axial, then turned by a vortex, and finally reattached to the upper wall, forming the captured gas region. In the

multi passage case, the inflow angle is larger, because the flow direction around the leading edge is almost circumferential, leading to the smaller captured gas region.

4 Conclusion

In this study, wave rotor inner flow dynamics were investigated both numerically and experimentally.

Fundamental features relating the pressure wave dynamics and the structure of contact surface were firstly investigated in detail by adopting the single passage case, wherein the observation of the basic wave and flow phenomena was successfully achieved and a cross check of the results between the experiments and numerical simulations showed very good agreement, thus attaining some confidence in the present methodology.

The "gradual passage opening effect" was examined by comparing the results due to the different cell width, which clarified that this effect causes to weaken the primary shock wave development, as well as yields an influence upon the structure of the contact surface, leading to enhanced interference between the contact surface and secondary shock wave.

Multi passage effects are clearly observed in the interaction wave that was generated by the leakage from the neighboring cell at an instant of the primary shock reflection therein. Its intensity became almost that of the secondary shock wave when the clearance size was large. This effect was again confirmed by the experimental results. Furthermore, the numerical results showed that the incoming flow angle, as the cell starts opening to the Gas-HP, was much influenced by the multi passage effects, yielding due difference in the contact surface states.

References

[1] Welch G.E., Jones S.M., Paxson D.E., "Wave Rotor-Enhanced Gas Turbine Engines", NASA Technical Memorandum 106998, AIAA-95-2799, 1995

[2] Kentfield J.A.C. "Wave rotors and highlights of their development", AIAA98-3879

[3] Fatsis A., Ribaud Y., "Thermodynamic analysis of gas turbines topped with wave rotors", Aerospace Science and Technology, no.5, pp293-299, 1999

[4] Wilson J., Paxson D.E., "Jet Engine Performance Enhancement Through Use of a Wave-Rotor Topping Cycle", NASA Technical Memorandum 4486, 1993

[5] Nalim M.R., "Thermodynamic Limits of Pressure Gain and Work Production in Combustion and Evaporation Processes", AIAA-98-3398, 1998

[6] Akbari P., Muller N., "Preliminary Design Procedure for Gas Turbine Topping Reverse-Flow Wave Rotors", IGTC2003Tokyo FR-301 (CD-ROM), International Gas Turbine Congress 2003 Tokyo, Nov. 2003

[7] Paxson D.E., Wilson J., "An Improved Numerical Model for Wave Rotor Design and Analysis", AIAA-93-0482, 1993

[8] OKAMOTO K., NAGASHIMA T., " A Simple Numerical Approach of Micro Wave Rotor Gasdynamic Design", ISABE-2003-1213 (CD-ROM), 16th International Symposium on Airbreathing Engines, Aug. 2003

[9] OKAMOTO K., NAGASHIMA T., YAMAGUCHI K., " Introductory Investigation of Micro Wave Rotor", IGTC2003Tokyo FR-302 (CD-ROM), International Gas Turbine Congress 2003 Tokyo, Nov. 2003

[10] Welch G.E., "Two-Dimensional Computational Model for Wave Rotor Flow Dynamics", Journal of Engineering for Gas Turbine and Power, vol.119 978-985, 1997

[11] Larosiliere L.M., "Wave Rotor Charging Process: Effects of Gradual Opening and Rotation", Journal of Propulsion and Power, vol.11, No.1, January-February, 1995

[12] OKAMOTO K., "Wave Rotor Gasdynamics for an Aeropropulsion System", ICAS PROCEEDINGS 2000 No. 7.3.4 (CD-ROM) 22nd INTERNATIONAL CONGRESS OF AERONAUTICAL SCIENCES, Sep. 2000

[13] OKAMOTO K., NAGASHIMA T., YAMAGUCHI K., " Rotor-Wall Clearance Effects upon Wave Rotor Passage Flow", ISABE2001-1222 (CD-ROM), 15th International Symposium on Airbreathing Engines, Sep. 2001

[14] Wilson J., "An Experimental Determination of Losses in a Three-Port Wave Rotor", Journal of Engineering for Gas Turbine and Power vol.120 pp833-842, 1998